Measured Effects of Desert Varnish on the Mid-Infrared Spectra of Weathered Rocks as an Aid to TIMS Imagery Interpretation

Benoit Rivard, Shelley B. Petroy, and John R. Miller

Abstract—**The thermal infrared spectral properties (7–12 μm) of natural rock surfaces from Silver Lake, CA, are investigated. Although the reflectance of weathered rocks is largely a function of the quartz content in rocks, the presence of desert varnish (clay coating) on rocks reduces the reflectance and spectral contrast with features unique to the rock spectra persisting if varnish is thin. Thick varnish has a spectrum with a reflectance peak near 9.6 μm, due to clays, and resembles the spectra of clay-rich playa surfaces. Comparison of laboratory reflectance spectra for varnish and weathered rock samples, with TIMS emissivity spectra for Silver Lake, suggest that TIMS signatures for felsic rocks are dominated by weathered rock and rock debris. In contrast, it is likely that varnish plays an important role in the TIMS signatures of mafic rocks.**

I. Introduction

Desert varnish, which consists of mixed layer clay minerals with subordinate iron and manganese oxides [1], [2], [3], is an ubiquitous rock coating observed in deserts worldwide. Varnish is typically a few tens of micrometers thick [4], [5], but to the eye varnish can completely obscure the underlying bedrock. The stability of varnish on bedrock is related to the physical properties of the rock [5], properties which remain constant at a regional scale and control the proportions of weathered rock and varnished rock viewed by remote sensing systems [6]. In principle, varnish could obscure bedrock mineralogy to remote sensing systems because, typically, photon penetration in soils and rocks is restricted to a few hundreds of micrometers at visible and infrared wavelengths [7]. In practice, a recent study using Thematic Mapper data for the Meatiq Dome of the Eastern desert in Egypt [6] suggests that even heavily varnished and sediment-coated surfaces retain some reflectance information concerning the underlying rock types, although this information must still be used in conjunction with field observations for accurate lithologic discrimination.

In recent years, use of NASA's Thermal Infrared Multispectral Scanner (TIMS) for lithologic discrimination has been demonstrated for many areas. TIMS was designed to operate in the 8–12 μm thermal infrared atmospheric window because common rock-forming minerals have fundamental stretching and bending vibrations of Si-O bonds in this spectral region. The absorption features associated with the characteristic vibrations can be used as diagnostic signatures to infer rock compositions [8], [9]. If the penetration depth of radiation into the desert varnish layer is proportional to wavelength [10] then rock spectral signatures might be discerned in the TIMS spectral region (8–12 μm), even when obscured in the visible wavelengths. The work presented here evaluates this hypothesis for the area of Silver Lake, CA. As with the previous study of Thematic Mapper data for the Meatiq Dome, field observations are used to evaluate how the extent of bare rock and varnished rock relate to the physical properties of the rocks. These field observations are combined with laboratory reflectance spectra of selected samples and analysis of TIMS data to provide a basis for understanding the effects of desert varnish on rock discrimination in the mid-infrared region of the spectrum. The laboratory setting provides controlled conditions for the study of varnished surfaces in the absence of soil, vegetation, and atmospheric effects whereas the TIMS data provide the regional context of the study.

The results of this initial study are relevant to the geologic interpretation of TIMS data and terrestrial observations to be acquired by the Advanced Spaceborne Thermal Emission and Reflectance radiometer (ASTER) instrument which is an integral part of the Earth Observing System. In addition, the results of this study will be useful for future analysis of data to be acquired by the Thermal Emission Spectrometer (TES) instrument which is part of the Mars Observer Mission.

II. Field Study Area

Silver Lake is located east of Barstow in the Mojave Desert of California (Fig. 1). The lake surface is a playa of the dry type [11] and is ordinarily hard and mud-cracked. The climate is arid and hot; vegetation is very sparse. Precipitation averages 8 cm/yr and most of it falls in local summer downpours which produce flash floods. Desert varnish, which is thought to form where rainfalls do not exceed 25 cm/yr [12], is ubiquitous on rock surfaces around Silver Lake. Bedrock occurs along the west side and northern end of the lake. Extent of bedrock exposure varies with rock type and outcrops are extensively covered by rock fragments of local origin trapped in eolian deposits. The size of the fragments and the stability of varnish on bedrock are controlled by the physical properties of bedrock (presence of cleavage, scale of jointing, etc). Rock types

Manuscript received September 25, 1991; revised July 14, 1992.

B. Rivard and J. Miller are with the Earth Observations Laboratory, Institute for Space and Terrestrial Science, York University, North York, Ontario, Canada, M3J 3K1.

S. Petroy is with Labsphere Inc., North Sutton, NH 03260.

IEEE Log Number 9204715.

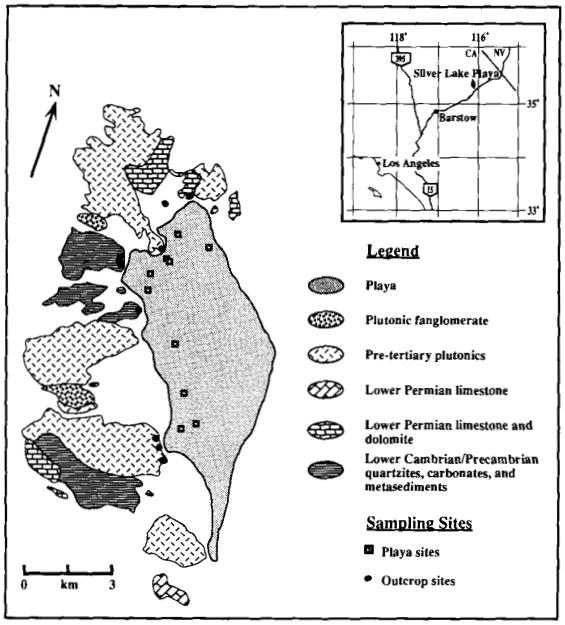

Fig. 1. Place map and lithologic map of the Silver Lake region. Ages of geologic units are discussed in [14]. Sampling sites are also shown.

observed in the area includes metasedimentary rocks and a complex of plutonic rocks ranging in composition from gabbro to granite (Fig. 1). Formation of thickest varnish is favored on stable rock substrates. For example, massive outcrops such as observed for gabbro are covered with thick and uniform varnish. In contrast, granitic rocks tend to exfoliate and weather to grus, and expose friable surfaces not stable for the development of varnish. As a result, varnish on granitic rocks is patchy and thin and outlines of bedrock crystals are visible despite the presence of varnish. Similar observations have been reported for other areas of the Mojave desert [5]. Varnish is also sparse on lithologies which form very smooth surfaces such as quartzite. Results from a previous study [13] suggest that smooth surfaces are not suitable for colonization by varnish-forming microorganisms.

All units previously mapped [14] (Fig. 1) were sampled with the exception of the fanglomerate and the lower Permian limestone. Samples were collected from the hills surrounding Silver Lake and the location of the sampling sites are shown on Fig. 1. The samples were medium to coarse-grained, 10 to 20 cm in diameter, and 10 to 15 cm thick. The rock surfaces collected for petrographic analysis and for laboratory acquisition of reflectance spectra had surfaces that are described as: 1) weathered, free of varnish, 2) freshly broken, or 3) varnished (Fig. 2). The mineral assemblages and abundance of minerals in these samples were determined from thin section petrography. Petrographic summaries for each rock type are given in Table I and were compared with published values for the same rock units [14]. Binocular observations of the weathered sample surfaces were acquired to complement the petrographic observations of the fresh rock because the reflectance signature of the samples is determined by the

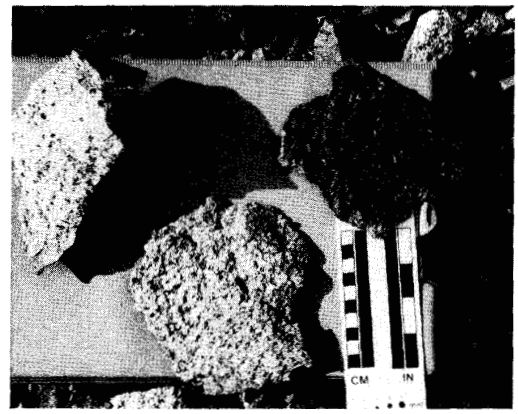

Fig. 2. Granodiorite samples: broken (left), weathered (center), and thinly varnished (right). Varnish on granodiorite is thin (10s of μm) and the outline of crystals from the substratum are commonly visible.

TABLE I
ESTIMATES OF MODAL MINERALOGY

blank	Qtz	Feldspar	Hbl	Bio	Px
Massive Quartzite	>99				
Granodiorite	40	>50, P>K		<10	
Bio-rich granite	40	40, P<K		20	
Qtz-monzonite	<10	>50	[40]		
Qtz-monzodiorite	15	40	15	30	
Gabbro	5	25	70		
Gabbro		50		20	30
Paragneiss:					
Qtz-rich layers: mostly feldspar and quartz with minor biotite and muscovite					
Qtz-poor layers: mostly biotite+phlogopite+muscovite with minor feldspar and quartz					

Qtz = quartz, Hbl = hornblende, Bio = biotite, Px = pyroxene. P = plagioclase feldspar, K = alkali feldspar.

mineralogy and texture of the surface layer a few 100's μm thick.

Samples of playa tile were collected from the Silver Lake playa to allow a comparison of playa tile and varnish reflectance spectra. The playa samples were on average 6 cm in diameter and 3–5 cm thick and consisted of individual tiles defined by adjoining mud cracks. During the sampling procedure and transport, care was taken not to disturb the top surface. X-ray diffraction spectra of powdered samples revealed that mixed clays (illite/montmorillonite) and quartz sand were the dominant mineral constituents of the tiles. Salts and carbonate minerals were observed locally.

III. VIEW FROM TIMS

A. Data Acquisition and Processing

The Silver Lake area was imaged by the NASA Thermal Infrared Multispectral Scanner (TIMS) on June 2, 1988, during

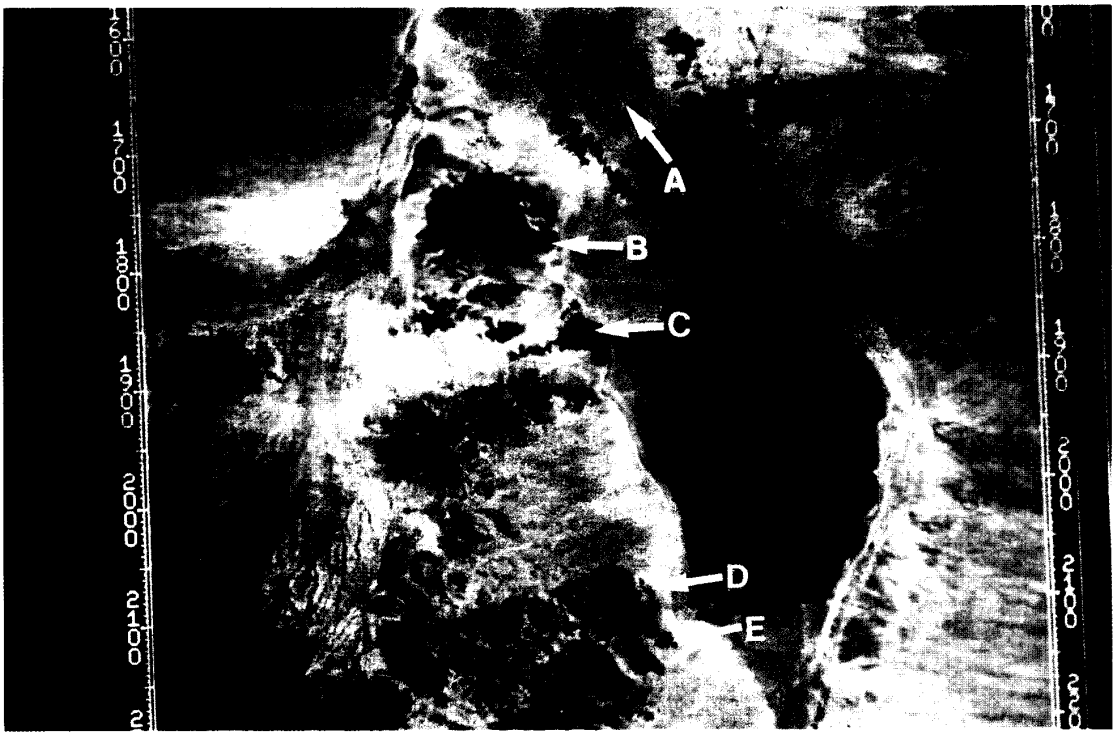

Fig. 3. TIMS image of the Silver Lake region. Decorrelation stretch bands 1, 3, and 5 are red, green, and blue, respectively. Arrows mark the locations of sampling sites for granite (A), quartzite (B), limestone (C), gabbro (D), and granodiorite (E).

the Mojave Field Experiment (MFE). TIMS acquires radiance data over six channels, which in 1988, were in spectral bands of: 8.2–8.6, 8.6–8.9, 9.0–9.4, 9.6–10.2, 10.3–11.1, 11.3–11.7 μm [15]. The instantaneous field of view is 2.5 mrad. Flight altitude was 8.2 km which provided a nadir ground resolution of approximately 20 m at the elevation of Silver Lake. The raw data is recorded in digital form and is converted to spectral radiance (mW m^{-2} sr^{-1} μm^{-1}) at the sensor through the application of a line-by-line calibration using signals from two internal blackbodies with controlled temperatures.

TIMS bands were then processed using decorrelation stretch procedures described in [16]. These procedures are based on principal component analysis and emphasize changes in emissivity as color differences while temperature variations are displayed as changes in intensity. Simple linear stretch of TIMS bands show mostly surface temperature variations and little variation due to lithology. Results from the decorrelation stretch depend on the frequency distribution of observed radiances, which vary from image to image. Nevertheless, previous studies [17]–[19], suggest that images enhanced using this approach have colors which relate in a predictable way to the spectral character of surfaces.

B. TIMS Images

A false color combination of decorrelation stretched bands 5, 3, and 1 mapped as red, green, and blue is shown in Fig. 3. This band combination maximizes discrimination of most felsic and mafic rocks at Silver Lake and was used in the field to guide selection and location of sampling sites. Field checking and use of the geology mapped by Grose [14] have shown a systematic relationship between colors on Fig. 3 and the distribution of rock units. This relationship must reflect in part the controls on spectral emittance of rock mineralogy, weathering styles, and extent of varnish and soil. The massive quartzite, which is mostly devoid of varnish, appears bright red. Carbonate rocks, such as limestone and dolostone, are free of varnish; in addition, carbonates are spectrally flat in the 8–11 μm wavelength region and appear green in this type of stretch. In contrast mafic rocks such as gabbros are extensively varnished and display a bluish-purple color. Rocks of intermediate composition, such as granodiorite, display a dull reddish-blue color. Color variations observed on the dry lake surface appear to reflect mostly mineralogical variations. Bright blue and purple areas of the lake consist mostly of compacted clays. Light blue-green areas reflect the influx of unconsolidated terrigenous sand material from local drainage. We found no field evidence of an anomaly to explain the bright green area observed on Fig. 3, for the south end of the lake. This area of the lake is the repository where water collects and evaporates last. A fragile crust of white carbonate material was observed locally in parts of the drainage where evaporation occurred recently. We speculate that this white material may have been widespread shortly after water evaporated from

the south end of the lake. It has been suggested that finely disseminated carbonate cement in the clay surface may be responsible for the green area in the image [20].

IV. Laboratory Spectral Measurements

This section presents results of laboratory spectral measurements on rock samples collected at Silver Lake. The results serve to estimate the spectral properties of the rock units observed in the field, and to provide constraints on the interpretation of TIMS data.

A. Procedure

An Analect Fourier Transform Infrared (FTIR) spectrometer, equipped with an integrating sphere attachment, was used to measure the hemispherical reflectance of the rock and playa samples. The sphere attachment is a hollow spherical cavity, the interior of which is coated with a rough gold surface. Port openings are provided for the incident radiant flux, photodetectors, and sample. The sample port is 2.5 cm in diameter. The samples are placed in the sample port of the hemisphere and are illuminated at 10° incidence angle by radiant flux from a heated nichrome wire source. Incident flux is first reflected by the sample and then randomly and multiply reflected by the sphere surface producing a uniform wall radiance allowing for a measure of the flux reflected into a hemisphere. The signal received by the detector is assumed to be dominated by light reflected from the surface because an intense thermal source was used to illuminate the sample surface. Thus the measurements are equivalent to directional- reflectance at a 10° zenith angle [21]. Spectral resolution within the 7–12 μm spectrum of interest is 4 cm^{-1}. Each analysis represents the average of 765 scans of the reflected beam from the sample divided by the average of 765 scans from the diffuse gold-coated standard. Each run takes approximately 15 min and provides an optimum signal to noise within a reasonable time frame. The playa surfaces were flat and placed directly against the sample port. Flat surfaces on rock samples were occasionally difficult to find and some signal loss may have resulted because these samples were not pressed tightly against the sample port. For coarse-grained rocks, repeated measurements were acquired and averaged to yield a representative spectrum of the rock.

For natural surfaces which are optically thick the emissivity in the thermal infrared can be derived from the reflectance using Kirchhoff's law [8], [22]–[24]. The form of Kirchhoff's law relevant to the measurements apparatus used in this work is:

$$\varepsilon(\Theta_O, \Phi_O; 2\pi) = 1 - R(\Theta_O, \Phi_O; 2\pi) \quad (1)$$

where $\epsilon(\Theta_o, \Phi_o; 2\pi)$ is the directional-hemispherical emissivity and $R(\Theta_o, \Phi_o; 2\pi)$ is the directional-hemispherical reflectance at a given wavelength. Assumptions of negligible sample thermal gradient and negligible radiant flux transmitted through the sample are believed to be valid given the thickness of the samples. In this study emissivity spectra were derived from the measured laboratory reflectance spectra using Kirchhoff's law because we aim to use laboratory reflectance spectra to interpret emissivity spectra derived from TIMS data. TIMS emissivity values were simulated for the laboratory samples by convolving the laboratory reflectance data at TIMS bandpasses with the response functions of the six TIMS channels.

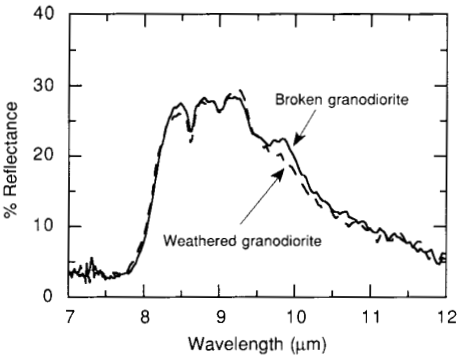

Fig. 4. Spectra of weathered (dashed line) and broken (filled line) granodiorite. Data are displayed as wavelength versus percent hemispherical reflectance.

B. Results and Interpretations

1) Effect of Varying Bedrock Mineralogy: Between 7–12 μm, interaction of thermal infrared energy with mineral grains, with grain sizes similar to that of our samples, produces reflectance maxima. Reflectance peaks for solid samples are also called "reststrahlen bands," and occur in the wavelength region of the fundamental Si-O stretching vibration, a resonant absorption frequency. The peaks occur because the extinction coefficient of the material is high with respect to the real part of the index of refraction which causes surface reflectance to dominate near resonance. The remaining penetrating radiation is absorbed just below the surface because the absorption coefficient is high.

Fig. 4 shows laboratory reflectance spectra for weathered and broken granodiorite. Note the overall similarity of these spectra. The spectrum of the weathered rock surface can, in this case, be used successfully to infer bedrock mineralogy. The three reflectance peaks between 8 and 9.5 μm are caused by quartz and feldspar, the dominant minerals in granodiorite. In the broken rock, the mineral biotite accounts for the reflectance peak at 9.9 μm. For the weathered surface, the corresponding peak is 3–4% weaker because: 1) biotite has altered to chlorite, a mineral with lower reflectance at 9.9 μm and, 2) because biotite and chlorite tend to be removed more readily by physical processes than quartz and feldspar. Fig. 5 shows laboratory reflectance spectra for a compositionally diverse suite of broken and weathered silicate rocks. Quartz-rich rocks (Fig. 5(a)) are characterized by high reflectivity (>20%) in the TIMS band 1 and 3 spectral regions. The overall trend for quartz-rich rocks is that of decreasing reflectivity with decreasing modal proportion of quartz. Quartzite displays the highest reflectivity values (>60%) and shows a set of bands centered near 8.5 and 9.2 μm characteristic of quartz [9], [25]. Granodiorite contains in excess of 50% feldspars (Table I) and its spectrum has a band near 9.2 μm because of

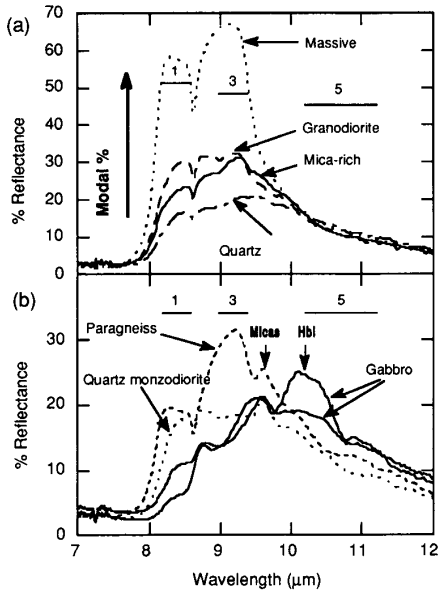

Fig. 5. Laboratory reflectance spectra for broken and weathered silicate rocks. (a) for quartz-rich rocks, (b) for quartz-poor rocks. TIMS channels 1, 3, 5 are also shown. "HBL" stands for hornblende. Note the different reflectance scales used on (a) and (b).

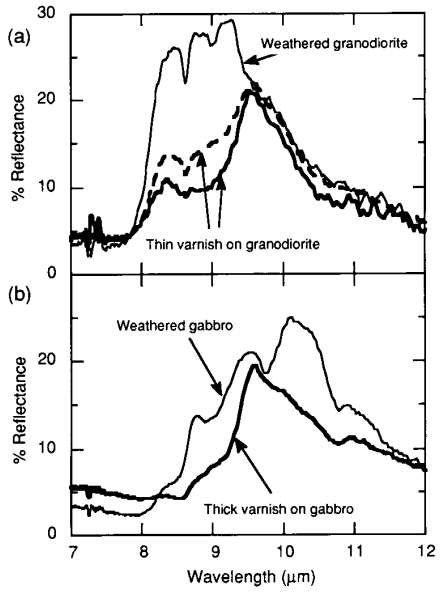

Fig. 6. Laboratory reflectance spectra for weathered and varnished rocks: (a) for granodiorite, (b) for gabbro.

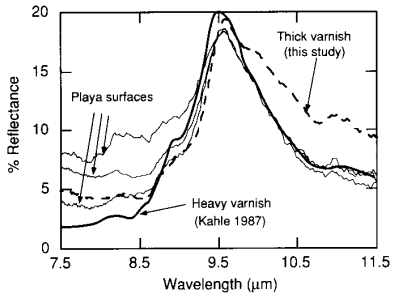

Fig. 7. Laboratory reflectance spectra of playa surfaces (thin continuous lines), of thick varnish on gabbro (thin dashed lines) from Silver Lake, and of heavy varnish (thick continuous line) on quartzite taken from [26].

feldspars. Compared with granodiorite, the mica-rich granite displays lower reflectance in the 8.2–9.2 μm region and higher reflectance from 9.2–9.9 μm. We speculate that these differences reflect the higher content of biotite and alkali feldspar in the granite. The quartz monzonite has a spectrum with uniform and low reflectance from 8.5–10.2 μm.

Quartz-poor rocks (Fig 5(b)) are characterized by low reflectivity (less than 20%) in the TIMS band 1 region. Rocks very poor in quartz (<5%), such as gabbro, have reflectivity which do not exceed 10% for the band 1 region. The spectra of gabbro are similar in shape but around 10.2 m, the hornblende-rich gabbro has a higher reflectance than the pyroxene-bearing gabbro. For these rocks maximum reflectivity occurs in the TIMS band 5 spectral region. Quartz-poor rocks display minimum and maximum reflectivity located at longer wavelengths than felsic rocks.

2) Effect of Varnish on Rock Spectra: Fig. 6 displays spectra of varnish on granodiorite and gabbro. Varnish on granodiorite is usually thin because granodiorite tends to weather rapidly by granular disintegration. Binocular observations show bright quartz and plagioclase crystals through the varnish. The spectrum of varnished granodiorite (Fig. 6(a)) displays a peak centered near 9.6 μm not observed on the spectrum of the varnished-free rock. This peak is characteristic of illite-smectite and/or kaolinite clays, the dominant constituents of varnish [1], [2]. The quartz doublet observed in the spectrum of weathered granodiorite is observed in the spectrum of thin varnish but as a weaker feature. Overall, the presence of varnish in granodiorite tends to reduce reflectance and contrast. Thick, uniform varnish is observed on gabbro, a massive rock type stable in comparison to granodiorite. When observed under binoculars, varnish on gabbro completely obscures the bright plagioclase crystals of the rock substrate. The spectrum of varnish on gabbro (Fig. 6(b)) has a peak centered near 9.6 μm due to clays. Short of 9.6 μm this spectrum lacks the presence of reflectance peaks observed in the spectrum of weathered gabbro. These features are due to plagioclase and their absence in the varnish spectrum suggest that varnish on our gabbro sample is optically thick short of 9.6 μm. Near 11 μm the varnish spectrum displays a hornblende band due to the reflectance contribution of hornblende either from the bedrock or as loose material entrapped in the varnish.

3) Playa Surfaces: Fig. 7 displays reflectance spectra for playa surfaces collected at Silver Lake playa. These surfaces consist of illite/smectite clays with subordinate quartz sand and their spectra are characterized by a symmetrical peak centered near 9.6 μm. The spectra of the playa surfaces are similar to the spectrum of thick varnish on gabbro. In detail thick varnish on gabbro has higher reflectance beyond 9.7 μm due to the presence of hornblende in the rock or entrapped in the

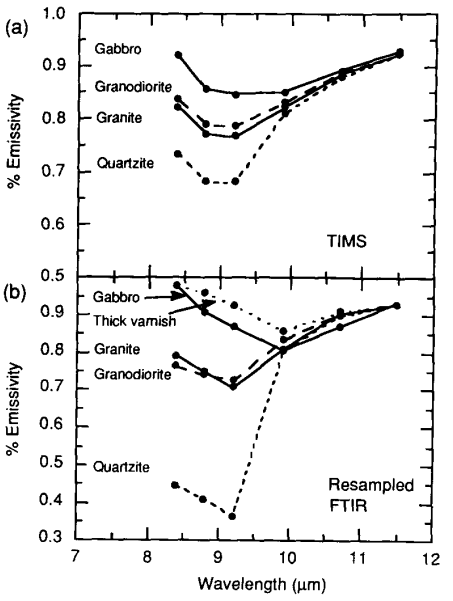

Fig. 8. Emissivity spectra for gabbro, granodiorite, granite, and quartzite rocks: (a) derived from TIMS data according to procedures described in Section V, (b) derived from laboratory FTIR reflectance spectra resampled to TIMS wavelength bandpasses, converted to emissivity using eq. (1), and normalized to TIMS band 6 value of 0.93. Also shown are results for thick varnish.

varnish. The spectrum of heavy varnish on quartzite published by Kahle [26] does not show this contamination effect by bedrock reflectance and compares well with the spectra of playa surfaces from Silver Lake throughout the 7.5–11.5 μm region.

V. Comparison to TIMS Spectra

Emissivity values were calculated from the TIMS data using the model emittance approach described by Kahle [27]. Because there are seven unknowns (six emissivities and the temperature) but only six radiance measurements, it is necessary to assume emissivity for one channel. For the felsic and mafic rocks of this study we assumed an emissivity value of 0.93 for channel six, an assumption which we feel is reasonable based on the comparison with our laboratory reflectance spectra. A temperature was then calculated for each picture element and used in conjunction with Planck's law to compute emissivity values for the other five channels. An atmospheric correction was applied using LOWTRAN-6 [28]. LOWTRAN allows the computation of emission and absorption by water and ozone, atmospheric constituents which contribute to the spectral radiance recorded by TIMS.

Atmospherically corrected TIMS six-value emissivity spectra (Fig. 8(a)) were extracted for the gabbro, granodiorite, granite, and quartzite sampling sites (see Fig. 3 for locations). These sites were chosen because they span a range of composition, and varnish and soil cover. The TIMS spectra describe large areas (20x20 m) including mostly outcrop and debris. These spectra can be compared with laboratory FTIR reflectance spectra collected from weathered rocks sampled from the same sites. For this purpose, the laboratory FTIR spectra of the weathered rocks were resampled to the TIMS wavelength bandpasses, converted to emissivity using Kirchhoff's law (1), and normalized to an emissivity value of 0.93 for channel 6 (Fig. 8(b)).

Differences in emissivity from rock to rock (Fig. 8(b)) are most apparent in bands 1, 2, and 3; these channels encompass the wavelength region corresponding to the major silicate absorption features. Both the laboratory and TIMS spectra show increasing emissivity values in channels 1 and 2 with decreasing quartz content of the rock and a concurrent shift in emissivity minima to longer wavelengths. This observation has been exploited quite successfully by several researchers using TIMS data for large-scale geologic mapping [7], [26], [29]. Note the similarity of the laboratory and TIMS spectra for granite and granodiorite (Fig. 8). These spectra display comparable contrast and emissivity values. Quartzite displays the spectra with highest contrast. The TIMS spectrum for quartzite has higher bands 1, 2, and 3 emissivity values compared to that of the laboratory spectrum for quartzite. The higher emissivity values of the TIMS spectrum are probably due to abundant quartzite debris in the field. As noted by several researchers [30], [31], the spectral contrast of reststrahlen bands decreases with decreasing particle size and increased porosity. The implication is that the TIMS signatures for quartzite, granite, and granodiorite outcrops appear to be largely controlled by the bedrock and debris mineralogy with little contribution from varnished surfaces, consistent with field observations. Thick varnish has a signature which resembles that of gabbro (Fig. 8(b)). As such, the effects of thick varnish on the gabbro TIMS spectra cannot be thoroughly evaluated without modeling TIMS emissivity using a suite of ground emissivity measurements of both weathered and varnished surfaces.

VI. Summary and Conclusions

The mid-infrared laboratory reflectance spectra for the Silver Lake samples provide a model for the effect of varnish on the TIMS signature of bedrock. For the samples of this study, the reflectance of weathered rocks is controlled by bedrock mineralogy. The most prominent reflectance variations observed for our sample collection is explained by varying quartz content. For samples displaying a varnish cover, the mineralogy of varnish also exerts controls on the reflectance of the rocks. In general, varnish tends to reduce the reflectance and spectral contrast of rocks. When varnish is thin, spectral features observed in the rock spectrum are preserved, but their magnitude is reduced. Laboratory spectra, collected from thick varnish on various rock types, display a relatively unique shape. Thick varnish show lowest reflectance in the wavelength region of TIMS band 1, 2, and 3, and a reflectance peak located near 9.6 μm. These features are also observed in the spectra of playa surfaces.

Field observations suggest that the thickness and extent of varnish is controlled by the physical properties of the rock substrate as was observed in other arid regions [5], [6]. Therefore, natural rock surfaces, when viewed by TIMS,

should display emissivity values weighted by proportions of varnish and weathered rock which depend on the rock type. The TIMS signature of granite, granodiorite, and quartzite are best explained by surface materials dominated by weathered bedrock and rock debris. These results are consistent with the presence of thin varnish and the general paucity of varnish on these rocks. In contrast, the TIMS signature of gabbro is similar to the TIMS signature of thick varnish simulated from laboratory reflectance spectra. Consequently it is not possible to ascertain the effect of varnish on the TIMS spectra of gabbro based on the study of laboratory spectra. However, in view of the widespread occurrence of thick varnish on this rock unit, it is likely that varnish plays an important role in changing the gabbro signature recorded by TIMS. A thorough assessment of this effect would require ground emissivity measurements.

The results suggest that varnish may modify the TIMS signature of mafic rocks. Consequently, use of TIMS data for the remote identification of mafic rocks should be conducted with care and when possible corroborated with field verifications. The remote identification of varnished mafic rocks with thermal infrared imagery can be facilitated knowing how varnish stability varies on the mafic rocks investigated. In addition, our FTIR spectra of gabbro and thick varnish suggest that higher spectral resolution may allow identification of features unique to various mafic weathered rocks and distinct from features of varnish. An instrument with spectral resolution greater than TIMS may therefore permit image analysis focused on locating areas where bedrock has little or no varnish. Crisp *et al.* [32] reached similar conclusions for their work on Hawaiian basaltic glasses.

ACKNOWLEDGMENT

Our thanks extend to Anne Kahle and Elsa Abbott of JPL for their discussions and logistical support. TIMS data was provided by Ray Arvidson at Washington University in St. Louis. Thermal infrared reflectance spectra were acquired using the FTIR facilities at JPL with the assistance of Joy Crisp. XRD analysis were provided by Cindy Grove at JPL.

REFERENCES

[1] R. M. Potter, and G. E. Rossman, "Desert varnish: the importance of clay minerals," *Science*, vol. 196, pp. 1446–1448, 1977.

[2] R. M. Potter, and G. E. Rossman, "The manganese and iron-oxide mineralogy of desert varnish," *Chemical Geology*, vol. 25, pp. 79–94, 1979.

[3] R. M. Potter, and G. E. Rossman, "Mineralogy of manganese dendrites and coatings," *American Mineralogist*, vol. 64, pp. 1219–1226, 1979.

[4] M. Sultan, R. E. Arvidson, N. C. Sturchio, and E. Guinness, "Lithological mapping in arid regions with Landsat thematic mapper data: Meatiq dome, Egypt," *Geological Society of America Bulletin*, vol. 99, pp. 748–762, 1987.

[5] R. I. Dorn, A. J. T. Jull, D. J. Donahue, T. W. Linick, and L. T. Toolin, "Accelerator mass spectrometry radiocarbon dating of rock varnish," *Geological Society of America Bulletin*, vol. 101, pp. 1363–1372, 1989.

[6] B. Rivard, R. E. Arvidson, I. J. Duncan, M. Sultan, and B. El Kaliouby, "Varnish, sediment, and rock controls on spectral reflectance of outcrops in arid regions," *Geology*, vol. 20, pp. 295–298, 1992.

[7] C. M. Pieters, "Strength of mineral absorption features in the transmitted component of near-infrared reflected light," *J. Geophys. Res.*, vol. 88, pp. 9534–9544, 1983.

[8] J. W. Salisbury, and L. S. Walter, "Thermal infrared (2.4–13.5 m) spectroscopic remote sensing of igneous rock types on particluate planetary surfaces," *J. Geophys. Res.*, vol. 94, pp. 9192–9202, 1989.

[9] J. W. Salisbury, L. S. Walter, N. Vergo, and D. M. D'Aria, *Infrared (2.1–25 m) Spectra of Minerals*. Baltimore: The John Hopkins University Press, 1992.

[10] C. Elachi, *Introduction to the Physics and Techniques of Remote Sensing*. New york: Wiley and Sons, 1987.

[11] D. G. Thompson, "Soda Lake and Silver Lake valleys," in *Playas and Dried Lakes: Occurrence and Development*, J. T. Neal, ed. USGS. Water Supply Paper 578, pp. 559–568, 1929.

[12] C. Elvidge, "Distribution and formation of desert varnish in Arizona," M. S. thesis, Arizona State U., Tempe, 1979.

[13] R. I. Dorn and T. M. Oberlander, "Rock varnish," *Progress in Physical Geography*, vol. 6, pp. 317–367, 1982.

[14] L. T. Grose, "Structure and petrology of the Northeast part of the Soda Mountains, San Bernardino County, California," *Geological Society of America Bulletin*, vol. 70, pp. 1509–1548, 1959.

[15] F. D. Palluconi, and G. R. Meeks, "Thermal infrared multispectral scanner (TIMS): An investigators guide to TIMS data," JPL Pub. 85–32, 1985.

[16] A. R. Gillespie, A. B. Kahle, and R. E. Walker, "Color enhancement of highly correlated images. I. Correlation and HSI contrast stretches," *Remote Sensing of Environment*, vol. 20, pp. 209–235, 1986.

[17] H. R. Lang, S. L. Adams, J. E. Conel, B. A. McGuffie, E. D. Paylor, and R. E. Walker, "Multispectral remote sensing as stratigraphic and structural tool, Wind River Basin and Big horn basin areas, Wyoming," *AAPG Bull.*, vol. 71, pp. 389–402, 1987.

[18] A. B. Kahle, A. R. Gillespie, E. A. Abbott, M. J. Abrams, R. E. Walker, G. Hoover, and J. P. Lockwood, "Relative dating of Hawaiian lava flows using multispectral thermal infrared images: A new tool for geologic mapping of young volcanic terranes," J. Geophys. Res., vol. 93, pp. 15 239–15 251, 1988.

[19] A. H. Collins, "Thermal infrared spectra and images of altered volcanic rocks in the Virginia Range, Nevada," *Int. J. of Remote Sensing*, vol. 12, no. 7, pp. 1559–74, 1991.

[20] S. B. Petroy, "Analysis of thermal infrared data acquired over playas: Silver Lake and Deep Springs Lake, CA, and Lunar Lake, NV," Ph.D. dissertation, Washington University, St. Louis, 1991.

[21] F. E. Nicodemus, "Directional reflectance and emissivity of an opaque surface," *Appl. Opt.*, vol. 4, pp. 767–773, 1965.

[22] E. Schanda, Physical Fundamentals of Remote Sensing. Berlin: Springer-Verlag, 1986.

[23] A. B. Kahle, M. S. Shumate, and D. B. Nash, "Active airborne infrared laser system for identification of surface rock and minerals," *Geophys. Res. Lett.*, vol. 11, no. 11, pp. 1149–1152, 1984.

[24] M. J. Bartholomew, A. B. Kahle, and G. Hoover, "Infrared spectroscopy (2.3–20 m) for the geological interpretation of remotely sensed multispectral thermal infrared dat," *Int. J. Remote Sensing*, vol. 10, pp. 529–544, 1989.

[25] J. W. Salisbury, L. S. Walter, and N. Vergo, "Mid-Infrared (2.5–25 m) spectra of minerals," First edition, USGS, Open-File Rep. no. 87–263, 1987.

[26] A. B. Kahle, "Surface emittance, temperature, and thermal inertia derived from Thermal Infrared Multispectral Scanner (TIMS) data for Death Valley, California," *Geophysics*, vol. 52, no. 7, pp. 858–874, 1987.

[27] A. B. Kahle, D. P. Madura, and J. M. Soha, "Middle infrared multispectral aircraft scanner data: Analysis for geological applications," *Appl. Opt.*, vol. 19, pp. 2279–2290, 1980.

[28] F. X. Kneizys, E. P. Shettle, W. O. Gallery, J. H. Chetwyn Jr., L. W. Abreu, J. E. Shelby, S. A. Clough, and R. W. Fenn, "Atmospheric transmittance/radiance: computer code LOWTRAN6," Air Force Geophysics Laboratory AFGL-TR-83–187, Environmental Research Papers, no. 846, 1983.

[29] A. R. Gillespie, and E. Abbott, "Mapping compositional differences in silicate rocks with six-channel thermal images", Proc. 9th Can. Symp. on Rem. Sens., St.John's, Newfoundland, pp. 327–336, 1984.

[30] G. R. Hunt, and R. K. Vincent, "The behavior of spectral features in the infrared emission from particulate surfaces of various grain sizes," *J. Geophys. Res.*, vol. 73, pp. 6039–6046, 1968.

[31] J. E. Conel, "Infrared emissivities of silicates: experimental results and a cloudy atmosphere model of spectral emission from condensed particulate mediums," *J. Geophys. Res.*, vol. 74, no. 6, pp. 1614–1634, 1969.

[32] J. Crisp, A. B. Kahle, and E. A. Abbott, "Thermal infrared spectral character of Hawaian basaltic glasses," *J. Geophys. Res.*, vol. 95, no. B13, pp. 21 657–21 669, 1990.

Benoit Rivard received the B.Sc. and M.Sc. degrees in geology at McGill University, Montreal, in 1983 and 1985, respectively. He received the Ph.D. degree in earth and planetary sciences from Washington University, St.Louis, MO, in 1990.

He is currently a project scientist at the Earth Observations Laboratory of the Institute for Space and Terrestrial Science (Toronto). His research includes the use of ground and airborne multispectral remote sensing for lithologic and structural mapping, applications of spectral unmixing techniques for mapping, the infrared characterization of terrestrial materials, and the development of methodologies for precise field measurement of emissivity.

Shelley B. Petroy received the B.S. degree in geology from the University of North Carolina, Chapel Hill, in 1983, and the M.S. degree in planetary geology from Arizona State University in 1985. She received the Ph.D. degree from the Earth and Planetary Sciences Department at Washington University, St. Louis, MO, in 1991.

After she graduated from the University of North Carolina, she spent 2 years as a research assistant with the Center for Earth and Planetary Studies, National Air and Space Museum, in Washington, DC. At Washington University, a significant portion of her dissertation research was conducted under the auspices of the NASA Graduate Student Fellowship Program. Her research focused on using thermal remote sensing as a diagnostic tool for identifying and mapping recent sediments and evaporites in the southwestern U.S. She is currently an Applications Scientist with Labsphere, Inc., NH.

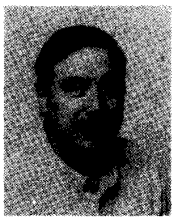

John R. Miller received the B.E. degree in physics from the University of Saskatchewan, Saskatoon, in 1963. He earned both the M.Sc. and Ph.D. degrees in space physics from the same university studying the aurora borealis using rocket-borne radiometers, in 1966 and 1969, respectively.

He then spent 2 years on a Postdoctoral Fellowship at the Herzberg Institute at the National Research Council in Ottawa. In 1971 he went to work as a Project Scientist at York University and obtained a faculty appointment in 1972. He is currently Professor of Physics & Astronomy at York University and is Co-Director of the Earth Observations Laboratory of the Institute for Space and Terrestrial Science. His remote sensing research interests have included interpretation of water color reflectance, atmospheric correction and canopy reflectance. Over the past 6 years his primary focus has been on the application of reflectance spectroscopic techniques in remote sensing using imaging spectrometers.